Topographic Indices and Two-dimensional Hydrodynamic Modeling for Flood Hazard Mapping in a Data-scarce Plain Area: A case study of Oued-Laou Catchment (Northern of Morocco)

Article *in* Geocarto International · May 2022

DOI: 10.1080/10106049.2022.2082548

CITATIONS
5

READS
423

7 authors, including:

Omayma Amellah
Università degli Studi di Parma
8 PUBLICATIONS **213** CITATIONS
SEE PROFILE

Karim El Morabiti
Abdelmalek Essaâdi University
19 PUBLICATIONS **239** CITATIONS
SEE PROFILE

Carmen Maftei
Transylvania University of Braşov
72 PUBLICATIONS **503** CITATIONS
SEE PROFILE

Constantin Buta
Ovidius University
21 PUBLICATIONS **78** CITATIONS
SEE PROFILE

Geocarto International

ISSN: (Print) (Online) Journal homepage: https://www.tandfonline.com/loi/tgei20

Topographic indices and two-dimensional hydrodynamic modelling for flood hazard mapping in a data-scarce plain area: a case study of Oued Laou catchment (Northern of Morocco)

Omayma Amellah, Karim El Morabiti, Carmen Maftei, Constantine Papatheodorou, Constantin Buta, Ali Bounab & Mahamat Ouchar Al-Djazouli

To cite this article: Omayma Amellah, Karim El Morabiti, Carmen Maftei, Constantine Papatheodorou, Constantin Buta, Ali Bounab & Mahamat Ouchar Al-Djazouli (2022): Topographic indices and two-dimensional hydrodynamic modelling for flood hazard mapping in a data-scarce plain area: a case study of Oued Laou catchment (Northern of Morocco), Geocarto International, DOI: 10.1080/10106049.2022.2082548

To link to this article: https://doi.org/10.1080/10106049.2022.2082548

GEOCARTO INTERNATIONAL
https://doi.org/10.1080/10106049.2022.2082548

Topographic indices and two-dimensional hydrodynamic modelling for flood hazard mapping in a data-scarce plain area: a case study of Oued Laou catchment (Northern of Morocco)

Omayma Amellah[a], Karim El Morabiti[a], Carmen Maftei[b], Constantine Papatheodorou[c], Constantin Buta[d], Ali Bounab[a] and Mahamat Ouchar Al-Djazouli[a]

[a]Department of Geology, Faculty of Sciences, Abdelmalek Essaâdi University, Tetouan, Morocco; [b]Departament of Building Services, Faculty of Civil Engineering, Transilvania University of Brasov, Brasov, Romania; [c]Department of Civil Engineering, International Hellas University, Thermi, Greece; [d]Department of Civil engineering, faculty of Civil Engineering, University Ovidius of Constanta, Constanta, Romania

ABSTRACT

This article aims to assess flood hazard in the Oued Laou basin. It is a catchment on the Mediterranean coast (Northern part of Morocco) potentially periled by flash floods and accelerated development of anthropogenic activities. In this study, two complementary methodologies were applied; the first one introduces a new topographic wetness index (TWI-Ks) that aims to identify flood prone-areas executed on the basin scale. Then were validated using sentinel-1 images. The second one is a two-dimensional (2D) hydrodynamic model applied on a locale scale (plain of Oued Laou), to describe and calculate the flood parameters and mapping flow indicators based on a high grid resolution (DTM) generated using Arial photogrammetry. The results highlight that the new approach of TWI-Ks model provides more reliable results than the classic TWI in terms of delineating areas at potential risk. Even though, both of them provide reliable susceptibility mapping. The analyses of the 200-year flood event simulated by 2D hydrodynamic HEC-RAS model, revealed that the flood inundation extent consequently affected almost all floodplain assets. Especially, crop fields and road N16, as tends to present danger even on buildings as a result.

ARTICLE HISTORY
Received 4 January 2022
Accepted 22 May 2022

KEYWORDS
Two-dimensional hydrodynamic models; flood modelling; high-resolution DEM; topographic indices; hazard map

1. Introduction

Natural hazards engendered by hydro-meteorological incidents, especially floods or river overflow, are one of the major hazards that lead to massive loss of human lives, interruption to transportation, utility services and properties each year (Kheradmand et al. 2018; Thapa et al. 2020). They are overtaking other disasters, both in the frequency of

CONTACT Omayma Amellah amellahoumaima@gmail.com; Carmen Maftei cemaftei@gmail.com

recurrence and damaging capacity throughout the world (Erena et al. 2018). For the period 2000–2015, flooding was the main cause of about 50% of all meteorological-related disasters, resulting in 2.3 billion human casualties (Geravand et al. 2020), 20.4% of the death toll and 19.3% of devastations, which represents around 40% of all-natural disasters, reaching the pinnacle of 70.1 billion US$worldwide (Fustos et al. 2017). In the future, and due to the global climate change, the frequency of extreme events may become more intense besides the increase of human activities, flood inundation hazard is predicted to be more damaging and disastrous (Jamali et al. 2018; Van Oldenborgh et al. 2018; Kossin 2018). These events themselves cannot always be predicted, their disastrous consequences can be considerably mitigated if areas prone to flood are carefully delineated previously, and flood risk measures are implemented accordingly (Yalcin 2020).

Prediction tools are efficient to forecast the behaviour of the flow process. However, they are based on many different proceedings and algorithms. They are customarily used as numerical models due to their ability to provide solutions for the mathematical equations that describe these flow mechanisms (Echeverribar et al. 2019). There are two main categories of numerical models with different capabilities to perform: first, hydrological/hydraulic analyses, including flood frequency analyses, regional methods, transfer methods, empirical method. Second, hydrodynamic routines for flood inundation and hazard potential resolving one-dimensional (1D), two-dimensional (2D), coupled (1D/2D) and three-dimensional (3D) flooding simulations (Gaume et al. 2009; Marchi et al. 2009; Sapountzis et al. 2021). A synergetic use of those models is recommended by many scientists (Komi et al. 2017; Teng et al. 2017), for this reason, this study emphasizes two approaches to flood management strategies from each category of flood modelling mentioned previously. Flood risk management work begins with the identification of likely areas of higher hazard potential based on a regional method (Plate 2002; Sanyal and Lu 2004; Forkuo 2011). Flood mapping determines the inundation extent by estimating water depth and velocity (Alaghmand et al. 2010) based on the 2D hydrodynamic model.

Regional methods are mainly based on geomorphologic indices. It has been employed to locate spatial soil wetness patterns (Burt and Butcher 1986; Moore et al. 1991) due to their limited parameterization requirements and uncomplicated formulation. The implementation of these indices can be efficient and provide reliable spatial information at regional scales while maintaining optimal accuracy. Such indices are specially carried out *via* their cumulative distribution (Buchanan et al. 2014). For instance, the topographic wetness index (TWI) is a suitable tool to estimate and predict areas prone to inundation. It was created for the first time by Beven and Kirkby (1979), through the runoff model TOPMODEL. This index can determine the influence of topography on runoff generation and is used as a physically-based index to define the spatial distribution of soil wetness (Beven and Kirkby 1979; O'Loughlin 1986; Barling et al. 1994). Furthermore, the use of TWI to locate flood susceptible areas at potential risk on a regional scale is a preliminary at which to apply in the second place hydraulic models to assess the potential risk on a local scale (Papatheodorou 2015). Due to their relevancy in term of simulating lateral flow dynamics under unsteady conditions, such as backflow in floodplains (Pinos and Timbe 2019). Among all hydrodynamic models, 2D simulations are seemed to be more adequate in resolving complex flood inundation processes on a local scale. Basically, 2D models simulate the distribution of water depth and velocity all over the expanse of a flooded zone through a grid or mesh representation that defines topographic information according to flood hydrographs integrated as upstream boundary condition (Yalcin 2020; Anees et al. 2017; Quirogaa et al. 2016).

Implementing several hydraulic/hydrodynamic modelling approaches to prevent the spatial variability of flood hazards demands modellers' intervention to supply considerable spatial details (high accuracy of the altimetric survey, optimum parameter values), which are not easily obtainable (Granados-Bolaños et al. 2021). These models also demand substantial setup and calculation time, typically with high-resolution waterway networks (Afshari et al. 2018). In our study area, The Oued Laou plain is an example of this situation. This latter, is becoming more and more vulnerable in terms of flash flood inundation owing to the constantly increasing rate of urbanization (Amellah et al. 2020). While a very gentle and flat topography makes it challenging to produce high-quality flood inundation maps. Recently, as a result of the advent of remote sensing technology, high-resolution digital terrain models (DTMs) have greatly improved, which will undoubtedly enhance the performance of hydrodynamic models. Many high-resolution satellite imageries provide centimetric accuracy (e.g. World View) but one of the difficulties is the accessibility to such data survey is hard to obtain due to the cost issues. Photogrammetry is an advantageous alternative in terms of generating high-quality of geomorphologic details with centimetric-scale resolutions owing to its benefits on time acquisition of high-resolution images, and cost-efficiency (Colomina and Molina 2014). It has been widely used in several hydrological researches on topographic analyses and natural hazards monitoring (Feng et al. 2015; Langhammer et al. 2017; Şerban et al. 2016; Quesada-Román et al. 2021).

The objective of this study is to assess and analyse flash flood risk of the Oued Laou River. It is potentially threatened by flash floods and an accelerated development of anthropogenic activities (on both banks of the River) besides a very large and extremely flat topography. These predispositions make the work of executing flood mapping strategies extremely challenging or impossible especially a simulation through a 2D hydrodynamic model. For this reason, and in order to ameliorate the anticipation of flood hazard information at study area, as Komi et al. (2017) mentioned both hydrological and hydraulic models are required. These two complementary flood modelling approaches were implemented. The first one leads to a susceptibility mapping to locate flood-prone areas on a regional scale based on TWI, and a new approach of TWI called TWI-Ks intended to be created to improve the classic model by integrating the hydraulic conductivity of the soil. In addition a parsimonious model in calculating and required data is judged as effective either for ungauged watersheds or for small sub-basins. The second one aims to produce Flood hazard maps and calculate the flood extent parameters (water depths, flow velocities and flood indicators) obtained in the unsteady flow simulations using a 2D hydrodynamic model established in HEC-RAS version 5.0 software, on a local scale. But before a high-resolution DTM has been generated using photogrammetry and frequency analyses of hydrological data related to the extreme flow event was necessary to proceed with the 2D simulation.

2. Material and methods

2.1. Study area

This study carried out in the Oued Laou River basin located between Tetouan and Chefchaouen Provinces (within the Mediterranean region) in northern Morocco at 35°25′60.0″N 5°04′45.4″W and 35°05′31.2″N 5°12′18.2″W (Amellah and El Morabiti 2021) (Figure 1).

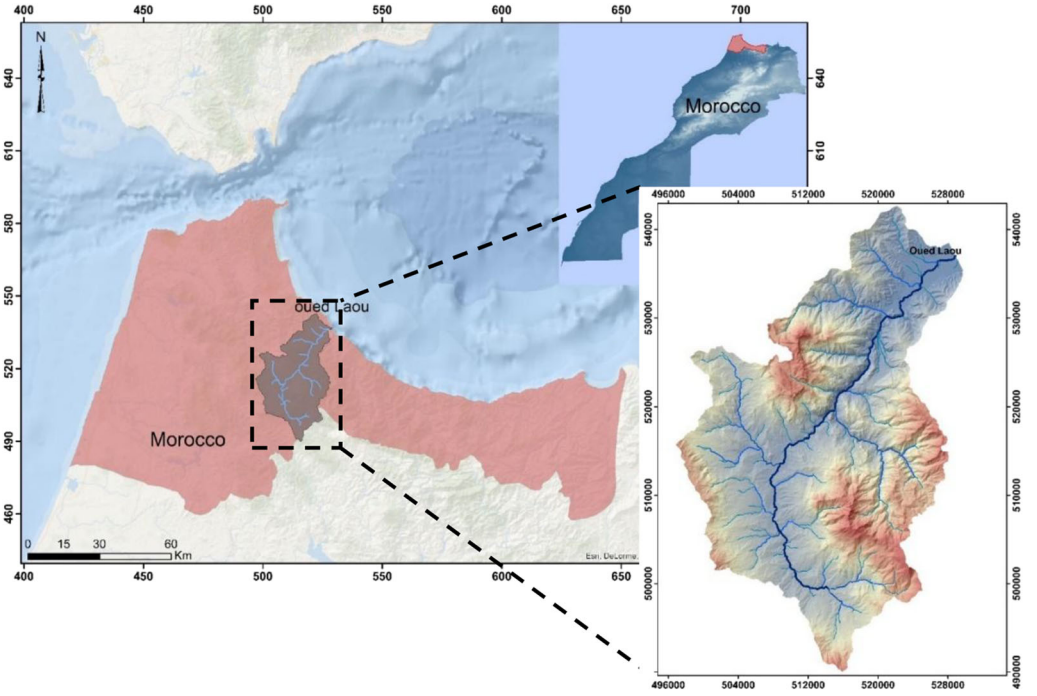

Figure 1. Layout map of the study site.

The study area comprises a river reach approximately 10 km long that flows across deep and narrow gorges (Oueslati 2008), with an average slope of 0.29%. The western floodplain comprises the commune urban of Oued Laou, while the eastern floodplain is mainly dominated by agricultural activities. The elevation is varying 0 and 2122 m with an average temperature of 18.6 °C and annual rainfall around 535 mm. This area was chosen because it is prone to frequent flooding.

2.2. Material and methods

In order to perform the flood modelling, and assess the flood risk in the Oued Laou watershed, two major approaches were followed at two different spatial scales of implementation. First, the application of a new approach of the TWI model on a regional scale in order to select exposed areas at flood risk. Second, based on the selected area by geomorphological approach at a regional scale, the 2D hydrodynamic model (HEC-RAS) was applied on a local scale to calculate the flood parameters (Figure 2).

2.2.1. Flood susceptibility analyses at a regional scale (basin-scale)

In order to generate the maps of areas susceptible to flood in the Oued Laou Pirimeter based on the TWI (TWI/SAGA-WI), a 5 m cell size resolution DEM was built from digitized contours of the official 1/25,000 topographic maps using GIS tools: indeed the contour features of four maps that covers the entire areas were revised and verified. Then they were merged manually and converted to a raster DEM using GIS tools. Then TWI and SAGA-WI was calculated as it is seen in (Figure 3).

The TWI was developed to anticipate prompt response flow by employing morphometric parameters (Moore et al. 1991; Sørensen et al. 2006). It can be adopted as a

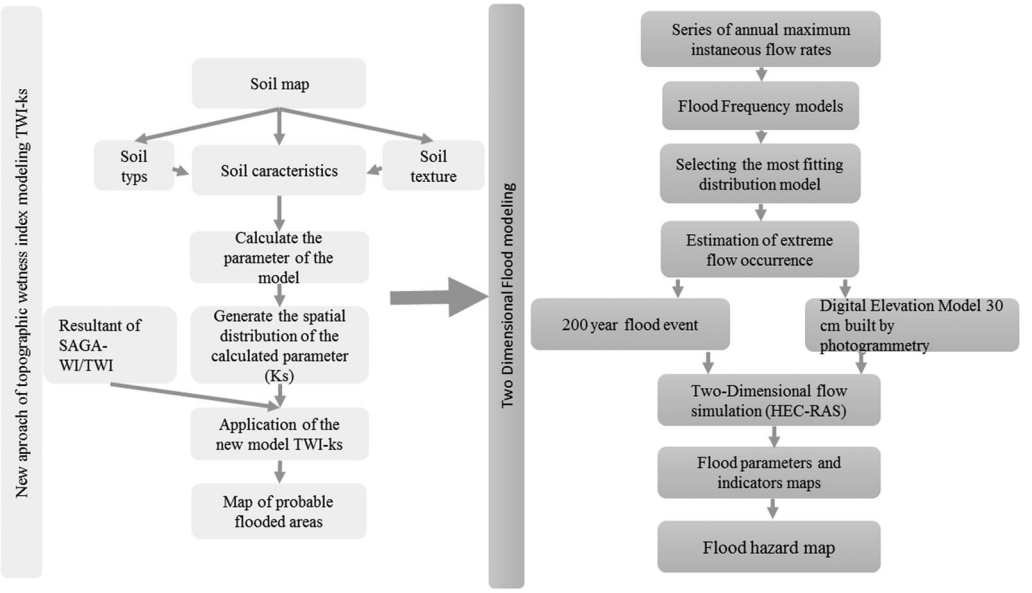

Figure 2. Scheme of work methodology.

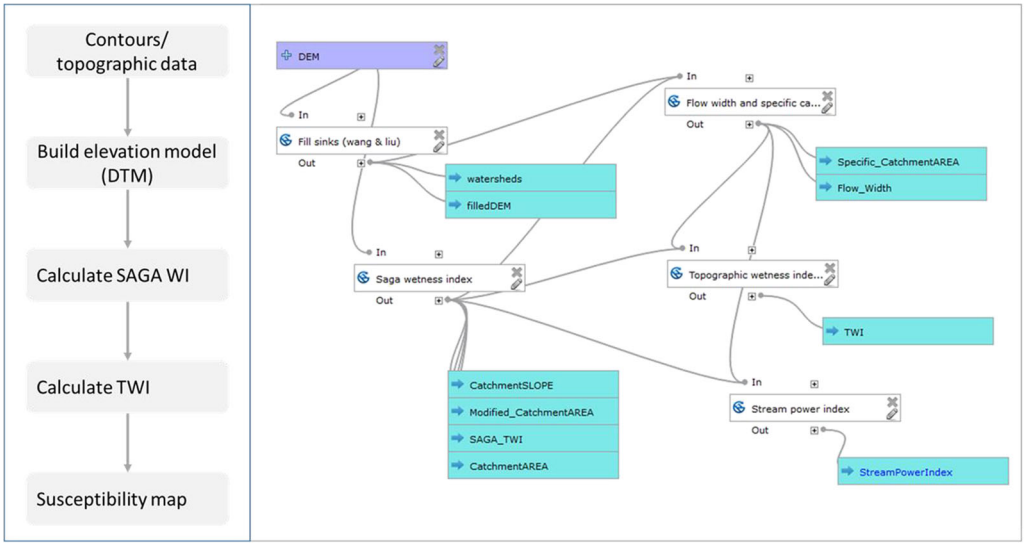

Figure 3. Scheme of TWI/SAGA-WI model Processing.

dependable method for precursory flash flood hazard assessment in cases where accurate hydrologic input data are scarce (Papatheodorou et al. 2015).

$$\mathrm{TWI} = \ln\left(\frac{A_s}{\tan(\beta)}\right) \tag{1}$$

where A_s = upslope contributing area per unit contour length (or specific catchment area [SCA]) and β = local slope gradient for reflecting the local drainage potential. The value of TWI is influenced by the algorithms to calculate α and estimate $\tan\beta$ (Guntner et al. 2004).

Table 1. The calculated hydraulic conductivity of each type of soil.

Soil types	Soil units	Hydraulic conductivity Ks (m/s)
Type 1	Slightly evolved Fersiallitic soils and Raw minerals	0.000006
Type 2	Slightly evolved soils	0.000008
Type 3	Fersiallitic and Slightly evolved soils	0.000005
Type 4	Raw mineral and Slightly evolved soils	0.000007
Type 5	Burnished and Slightly evolved soils	0.000006
Type 6	Calcimagnesic, Fersiallitic and Raw miniral soils	0.000005
Type 7	Burnished and Raw mineral soils	0.000006

The aim of this section is to introduce a new updated version of TWI. Many authors have tried to improve the TWI model with different approaches, by modifying the parameters of the basic equation, for instance Hjerdt et al. (2004) modified the concept of the slope by taking into consideration the distance. Also Quinn et al. (1991) integrate the multiple-flow-direction (MFD) algorithm first. Qin et al. (2007) proposed a new adapted (MFD-md), and applied it in Qin et al. (2011). Along the same lines, we also find the contributions of Böhner and Selige (2002), Yong et al. (2012) and Manfreda et al. (2011). All those researchers have worked on the improvement of the TWI, which inspired us to propose our own new approach called TWI-Ks that aim to enhance the performance, parameterization, and algorithm calculation of the TWI and also the need for a parsimonious model in calculating and required data. Since *in-situ* recordings over the entire basin are not always available or not accurate, especially for flash floods. This type of flooding is triggered by intense local storms and leads to short-term flooding especially in tributaries where the flow is not permanent. This type of model is most effective either for watersheds on a regional scale or for small sub-basins. As TWI quantifies the impact of the land relief on flow generation (Pourali et al. 2016). The main equation has been maintained as it is, and then the effect of soil has been integrated through the *Ks* parameter (2), where *Ks* is the hydraulic conductivity of the soil (Table 1). Since this latter is an important variable in mathematical models that anticipates soil hydraulic attitude. It describes water dynamics in soil profile (Laio et al. 2009). In so far as low *Ks* increases surface flow while high *Ks* engender high infiltration.

$$\mathrm{TWI} - \mathrm{K_s} \;= \ln\left(\frac{\mathrm{As}}{\tan\ (\beta)}\right)\mathrm{K_s} \tag{2}$$

where A_s = the upslope contributing area per unit contour length. β = local slope gradient for reflecting the local drainage potential. *Ks* = the hydraulic conductivity of the soil.

Soil data were provided by the Provincial Directorate of Agriculture of Tetouan (PDA) including soil map (Figure 4), soil characteristics and measurements.

Soil characteristics of the Oued Laou Basin can affect the process of flow generation. According to the soil map, there are seven types of soil, its texture varies between fine to medium, depends on the apportionment of the percentage of silts, clay, and sand in each type of soil, which consequently controls the soil drainage.

In order to validate the new model, the TWI-Ks model was calculated and compared with TWI/SAGA-WI and a real flood event that affected the Oued Laou plain during the first week of March 2018. The two images used for mapping the event were retrieved from ASF DAAC in 25/09/2021. The first scene which documents the extent of water bodies before the event (permanent water bodies), was acquired in 15/02/2018, while the second was captured in 05/03/2018, during the flooding event. To process the two scenes, we used the open-source Sentinel Aplication Plateform freely available of the European

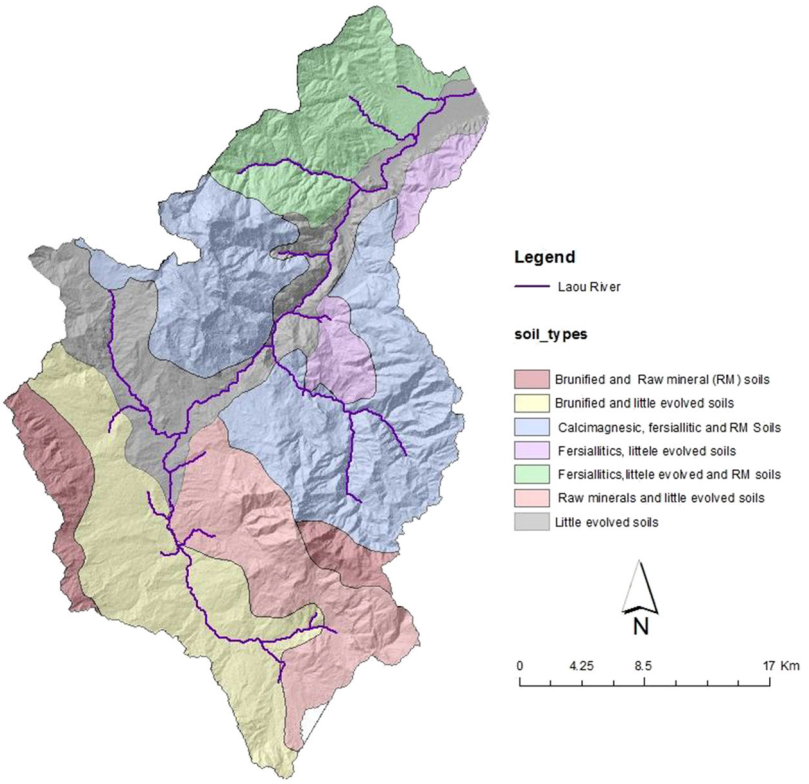

Figure 4. Map of soil types modified from the official soil map of the RIF (2000).

Spatial Agency's (ESA) website. Details about the processing chain and theoretical principles supporting this approach are detailed by Bărbulescu and Maftei (2021).

2.2.2. Flood analyses at locale scale (the downstream floodplain)

The flood frequency analyses aim to predict the return period of extreme flow events. The hydrological data used in this section includes annual instantaneous maximum discharges recorded at the Koudiat Kourriren hydrometric station. Collected over 48 years 1970–2018. This data were delivered by the Basin Lokkous Hydraulic Agency. Then was exploited to predict the return periods of extreme runoff events in the study area catchment. The frequency analysis of flow rates extremes implies adjusting a probability distribution to the observed input, to pertinently calculate the frequency of occurrence of extreme events (Keller et al. 2012; Zuhlke et al. 2015). For this reason, maximum values of the instantaneous annual flow rates were fitted to 10 of the most commonly used in hydrological analysis, probability distributions. To select the most adequate probability distribution for our observed data we have opted for the well-known AIC and BIC criteria given its wide application in hydrology.

- (AIC) Akaike information criterion (Akaike and Csaki 1973):

$$\mathrm{AIC} = -2\,\mathrm{Ln}\,(\mathrm{L}) + 2\mathrm{k} \tag{3}$$

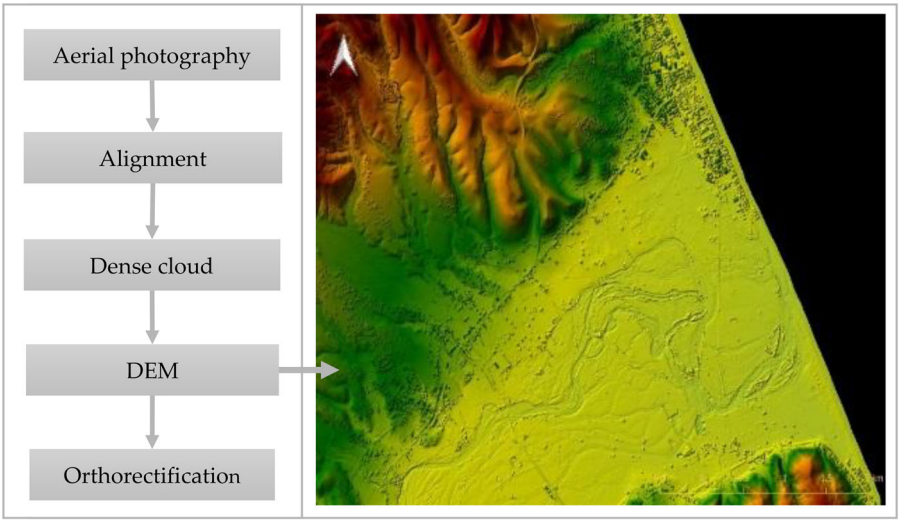

Figure 5. 30 cm resolution DEM process generation for the Oued Laou floodplain.

Table 2. System and processing information of Aerial photos.

Item	Description
Flight height	2355 m
Average pixel size	15 cm
Image size	17310*11310
Ascending yaw	−56 ± 0.5
Descending yaw	123 ± 0.5
Pitch and roll	0 ± 0.5
Aquisition date	9 December 2017
Number of images used	117
Processing software	Alice Vision Meshroom

- (BIC) Bayesian information criterion (Schwarz 1978):

$$\mathrm{BIC} = -2\,\mathrm{Ln}\,(\mathrm{L}) + \mathrm{k}\,\mathrm{Ln}\,(\mathrm{n}) \tag{4}$$

where L is the maximized value of the likelihood function, k is the number of estimated parameters of the model and n is the number of observation.

Producing high-quality altimetry data (DEM) using aerial photogrammetry to predict the flood inundation risk is an adequate alternative for flood assessment since the LiDAR/satellite-based remote sensing technologies cannot be used due to cost issues. High spatial resolution DEM – 30 cm cell size resolution – (Figure 5) was generated from photogrammetry technique: indeed, 117 aerial photographs (15 cm) supplied by the Urban Agency of Tetouan (Table 2), was used to produce a high-resolution DEM (30 cm). The absence of a dense forest canopy facilitated the use of this technique since the filtering of points from the dense cloud was not needed. The vertical error was then corrected using 25120 Ground Control Points (GCPs), to reduce the latter to 0.85 m. Also a high resolution (15 cm) Orthorectified image was produced from the data.

In order to map flood parameters and hazard levels in the Oued Laou plain, the hydraulic model selected to simulate the extreme of high flow rates of this study is the HEC-RAS model created by the U.S. Army Corps of Engineering (USACE). The latter solves the 2D diffusive equations wave or the 2D Saint-Venant equations) (Brunner 2010; Patel et al. 2017). The modelling process, in HEC-RAS version 5.0 software using the 2D

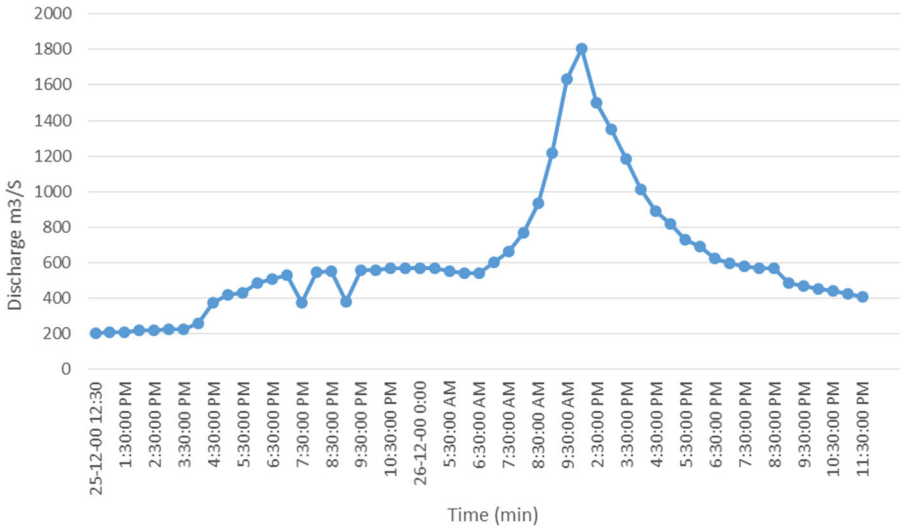

Figure 6. Flood hydrograph of the real event recorded on December 2000.

hydrodynamic model: the terrain elevation (30 cm cell size resolution) and orthophoto produced previously were first integrated into the RAS Mapper of the software, which leads to drawing the 2D flow area that includes all zones probable to be under risk, then a 2D mesh has been generated from the data automatically at this level. The next step consisted of integrating the upstream and downstream boundary conditions. For the upstream boundary condition line, the flow hydrograph was used (Figure 6) to generate flow in the simulation area. Regarding the downstream boundary condition, the normal depth type boundary condition was utilized (0.003).

The next step before starting the simulation within the Unsteady Flow Analysis editor is the attribution of Manning's roughness values for each land use type based on the land cover layer in the 2D flow area. The roughness values are attributed respectively as 0.020, 0.030, 0.050, 0.150, 0.035 and 10 for the roads, bare soil, water, trees, grass classes and buildings (Chow 1959).

The calibration of the model carried out based on the Manning coefficient and the discretization of meshing while adjusting its cell size. Thus, we called for a heterogeneous meshing to obtain a mesh adapted to the specificities of our site, which was detailed in Bomers et al. (2019). Considering the lack of past flood records solicited for model calibration, it was aimed to use very high-resolution datasets in model development. Thus, to more precisely simulate the flood flow movement as it was mentioned by Yalcin (2020): indeed the use of real instantaneous flow measurements (pic 1800 m^3) and 30 cm resolution of elevation datasets were sufficient for the model to be calibrated.

3. Results

3.1. TWI and new approach of TWI (TWI-ks)

Figure 7 shows the distribution of the wetness index over the entire basin outcomes obtained by TWI and SAGA wetness index. Patterns with low value of TWI are represented as green grids on the map which corresponds to dry areas, however, wetlands subject to overland flow displayed as blue patterns. TWI and SAGA-WI values swing between 2 and 9. The area's most susceptible are those located around the water

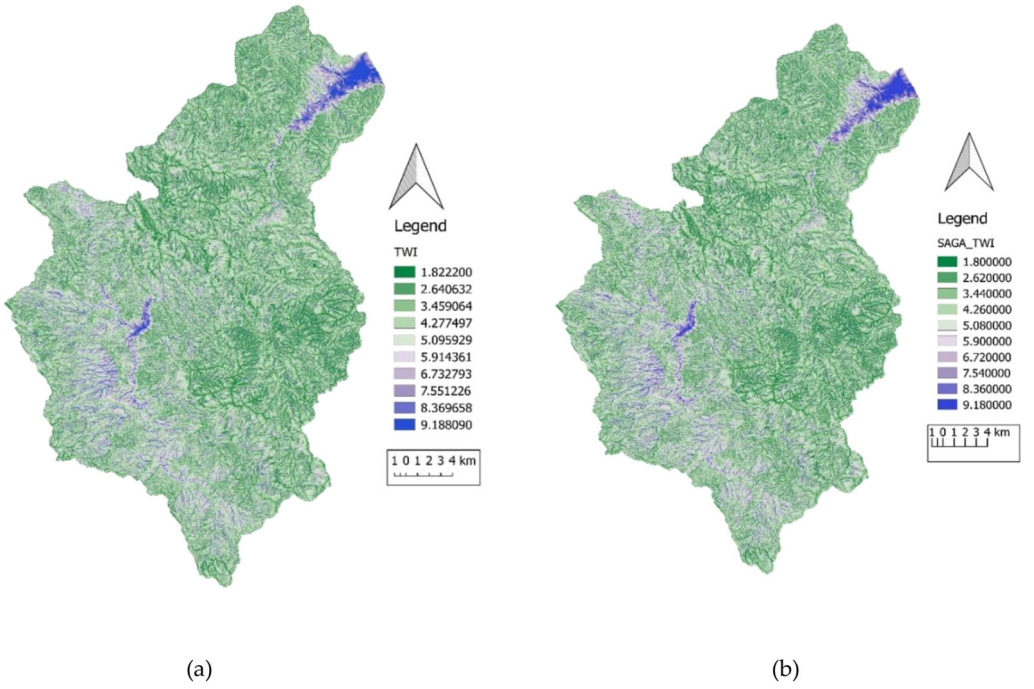

(a) (b)

Figure 7. TWI results (a) flood-prone areas predicted by TWI, (b) flood-prone areas predicted by SAGA-WI for Oued Laou Catchment.

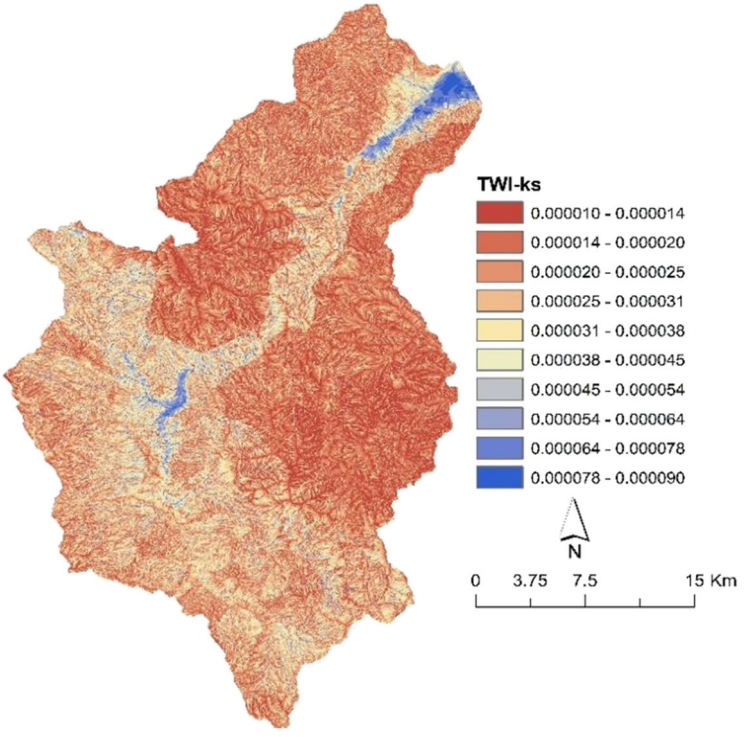

Figure 8. Results of the new model of TWI (TWI-ks).

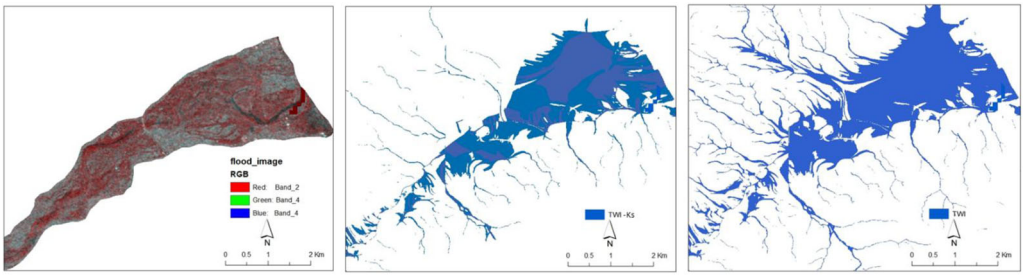

Figure 9. Comparison of (a) real flood image with (b) TWI-Ks and with (c) TWI.

pathways, at the edge of the dam where the values vary (7–9) and downstream to the flood plain.

The new approach of TWI (TWI-Ks) aimed to enhance the performance of the previous results predicted by TWI/SAGA-WI. As the results shown in Figure 8, the TWI-Ks tend to generate less number of wetlands in the middle and downstream the watershed. Whereas upstream and around the river pathway show more blue patterns and consequently, high susceptibility. Which can be interpreted by the effect of soil characteristics integrated into the model that has adjusted the spatial flow genesis results. Quantitatively TWI-Ks values oscillate between 0.00001 (no susceptibility) and 0.00009 (extremely high susceptibility).

Figure 9 compares the results of both topographic indices with a real flood event presented by a remotely sensed Sentinel-1 images. This event was recorded on March 2018. The comparison shows a clear difference between the basic TWI and the new approach TWI-Ks, in terms of the wetland distribution and estimation. Indeed, the fraction of wet patterns predicted by TWI and SAGA-WI tends to be overestimated. While the wet landscape predicted by TWI-Ks tends to be more realistic with less wet patterns which reflect the effect of the soil all over the basin. Regarding the delineation of the flood prone area was typically large based on the predictions given by TWI. While it is clearly optimized by the new perspective TWI-Ks. Insofar as the definition of the areas prone to floods is appearing more refined, especially at the downstream floodplain. All the topographic indexes applied over this basin as regional analyses reveal that the area most likely to be flooded is the part downstream of the Laou River. Consequently, it is the area that has been selected to implement on a second stage the 2D hydrodynamic model for local assessment (flood plain scale).

3.2. Flood frequency analysis

In order to select the most adequate probabilistic distribution for the hydrological dataset, the series of observations have been adjusted by 10 frequency distributions which gave initially a graphical description of extreme floods (Figure 10). But before that, the annual instantaneous maximum discharge data, referring to a large period of records (48 years), has been prepared. The latter is between 1970 and 2018 without gaps or missing records.

A preliminary comparative analysis of the real observations against the simulated curve was accomplished, as it is shown in the graphical representation of the frequency models considered. Among all the models were applied, the Pareto statistic graph shows the optimal fitting for our series of discharge. The Pareto distribution has been suggested for the assessment of flood magnitudes (Wang 1991). To confirm and reinforce the graphical

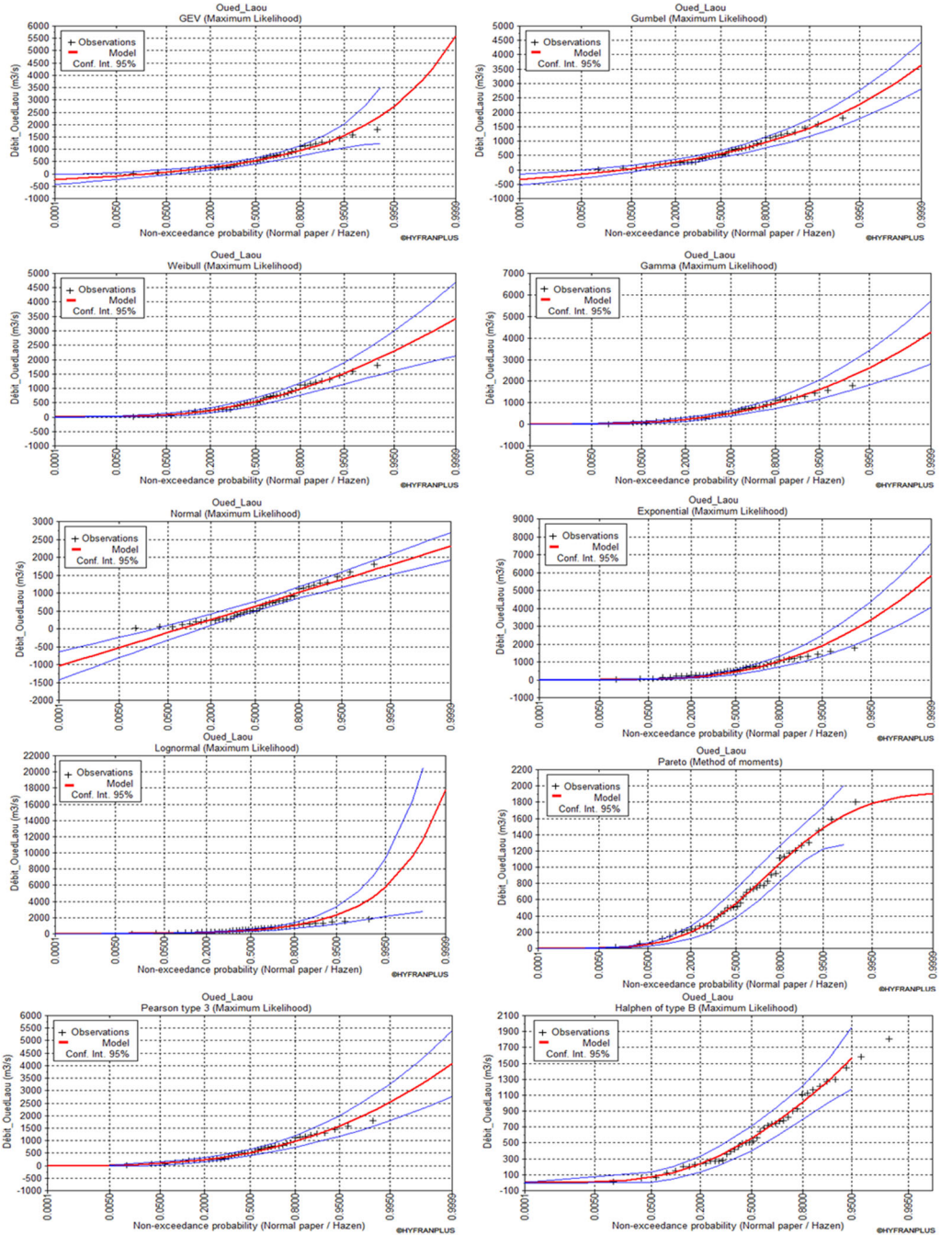

Figure 10. Graphical results of the observation adjustment by 10 probabilistic distribution.

results, we called for the AIC and BIC criterias, which allows to identify the most adapted models for observed data (Kuha 2004). The result values of these criteria are arranged in ascending order in Table 3. The model that has the lowest value for both AIC and BIC corresponds to the most suitable distribution, which in this case is the Pareto distribution. Thus, the criteria confirmed our expectations based on the graphical method.

Table 3. Criteria of choosing the fitting distribution.

Law	Number of parameters	Discharge (m^3/s)	BIC	AIC
Pareto	**2**	**1724.85**	**626.287**	**622.812**
Weibull	2	2076.736	627.265	623.79
Gamma	2	2318.278	628.356	624.88
Halphen of type B	3	2320	630.355	625.142
Gumbel	2	2024.926	631.825	628.349
Pearson type 3	3	2250.425	631.958	626.745
Exponential	2	2920.819	633.515	630.04
GEV	3	2351.872	635.102	629.889
Lognormal	2	4487.461	637.857	634.382
Normal	2	1680.79	638.878	635.402

Highlighted values given by the Pareto distribution that were selected to adjust the discharge dataset among 10 frequency distribution. This distribution that showed a maximum fit to the used data.

Table 4. Occurrence by Pareto distribution.

T = year	Frequency	Discharge (m^3/s)
1000	0.999	1860
200	**0.995**	**1780**
100	0.99	1720
50	0.98	1640
20	0.95	1480
10	0.9	1300
5	0.8	1050
3	0.6	802
2	0.5	554

Bold refers to the values of the discharge during an extreme flood event that its period of return is 200 year. it is the period of return that were selected for 2d simulation.

Flood frequency models have been employed by Smith (1989) to guesstimate recurrence intervals of maximum floods. In our study area, and after the analysis of the annual maximum instantaneous flow series, the maximum event that has been recorded during 48 years is the one related to December 2000 with a peak of 1800 m^3/s. The 200-year occurrence given by Pareto distribution as it is represented in Table 4 is 1780 m^3/s, since the estimated discharge is relatively close to the observed one we decided to proceed with the real event of December 2000.

3.3. Spatialization of 200-year flood inundation through 2D hydrodynamic modelling

Figure 9(a) shows the variation of the flood depth Water Surface Elevation, and Velocity occurred on 26 December 2000 at 00:30 (peak of the hydrograph). The minimum depth of flood highs is 1 cm simulated in the outskirts of the flood plain, whereas in the main channel, it reaches 7.8 m. Those highs lead to bridge submergence, the latter situated on the road N 16 that connects between Oued Laou and Kaâ Assras city. The bridge is 3 m high while the water depth in the same location is about 6,77 m.

Moreover, such events emerge almost all of the cultivated fields on both sides of the river. Figure 9(b) Illustrates that in the majority of these flooded landscapes, the water velocity is lower than 2 m/s. Such low values of water speed don't present a high hazard to the assets surrounding the river banks. Which is interpreted and kind of expected by the topographic predispositions of the site. Figure 9(c) shows the distribution of the lateral expansion of water/water surface elevation. The surface is vast and occupies almost the entire flood plain. As the altimetry variation in the watercourse of the river tends to zero, and the flow is extreme, water covers the maximum of space.

Table 5. Indicators Vis their equations.

Indicator	Equation
Energy head	$Eh = h + v^2/2g$
Indicator for flow force	$IFF = h * v^2$
Intensity	$I = v * h$

Table 6. Thresholds for mapping hazard indicators.

Indicator	Water depth (m)	Flow velocity (m/s)	Intensity (m^2/s)
Low	0–0.60	0–0.60	0–0.36
Medium	0.60–1.20	0.60–1.20	0.36–1.50
High	>1.20	>1.20	>1.50

Using HEC-RAS and GIS software, some hazard indicators have been mapped such as energy head (Eh), indicator for flow force (IFF), intensity (I) (Tables 5 and 6) to define the hazard levels in the flood plain of Oued Laou Basin as it is shown in Figures 11 and 12). The distribution of the maximum values of the three indicators is situated in the mainstream while decreasing in borders. The intensity varies between 2 and 12 throughout the floodplain. Energy Head shows a minimum of 1.4 towards the outskirts of the flooded area and a maximum of 32 inside the main river. The most represented values are between 3 and 8 for the majority of the flood extent area. Regarding IFF reveals a maximum of 30 for deep water, however, a minimum of 0.2 relates to shallow water.

Figure 13 shows three levels of hazard were in Oued Laou plain. The red feature corresponds to the highest level of hazard. And consequently the area with the serious apparent damages. The medium and low hazard features are located at the limit of the city and the floodplain. Generally, the 200-year inundation covers and damages all the crop fields situated on the floodplain and national road number 16.

4. Discussion

4.1. Flood susceptibility analyses at a regional scale by TWI and TWI-ks

SAGA wetness index is an analogue version of TWI (Maftei and Papatheodorou 2015) that predicts more reliable soil wetness than TWI (Maftei and Papatheodorou 2015). The results interpretation reveals that the areas most likely to be flooded are situated at low reliefs, low slope landscapes, towards the downstream catchment represented by a large blue pattern on the map. This reflects the important effect of topography as a key parameter of this model which controls the flow distribution in the basin. This quantitative approach based on morphometric indices has provided and visualized more detailed outputs analyses when spatial variability of soil properties has been included into the algorithm calculations.

The new approach of TWI (TWI-ks) delineated flood-prone areas effectively. The previous results predicted by TWI/SAGA-WI have been enhanced remarkability by TWI-ks. And then the performance of the model accordingly. This can be interpreted by the effect of soil characteristics integrated into the model that has adjusted the spatial flow genesis process.

The reliability of the model outcomes was tested and compared to a real flood mask and to the well-known TWI and SAGAWI outputs. TWI-ks provides a good performance in terms of quality mapping better than the TWI which reflects the effect of the soil conductivity all over the basin. And its importance as a key parameter in flood geneses. The

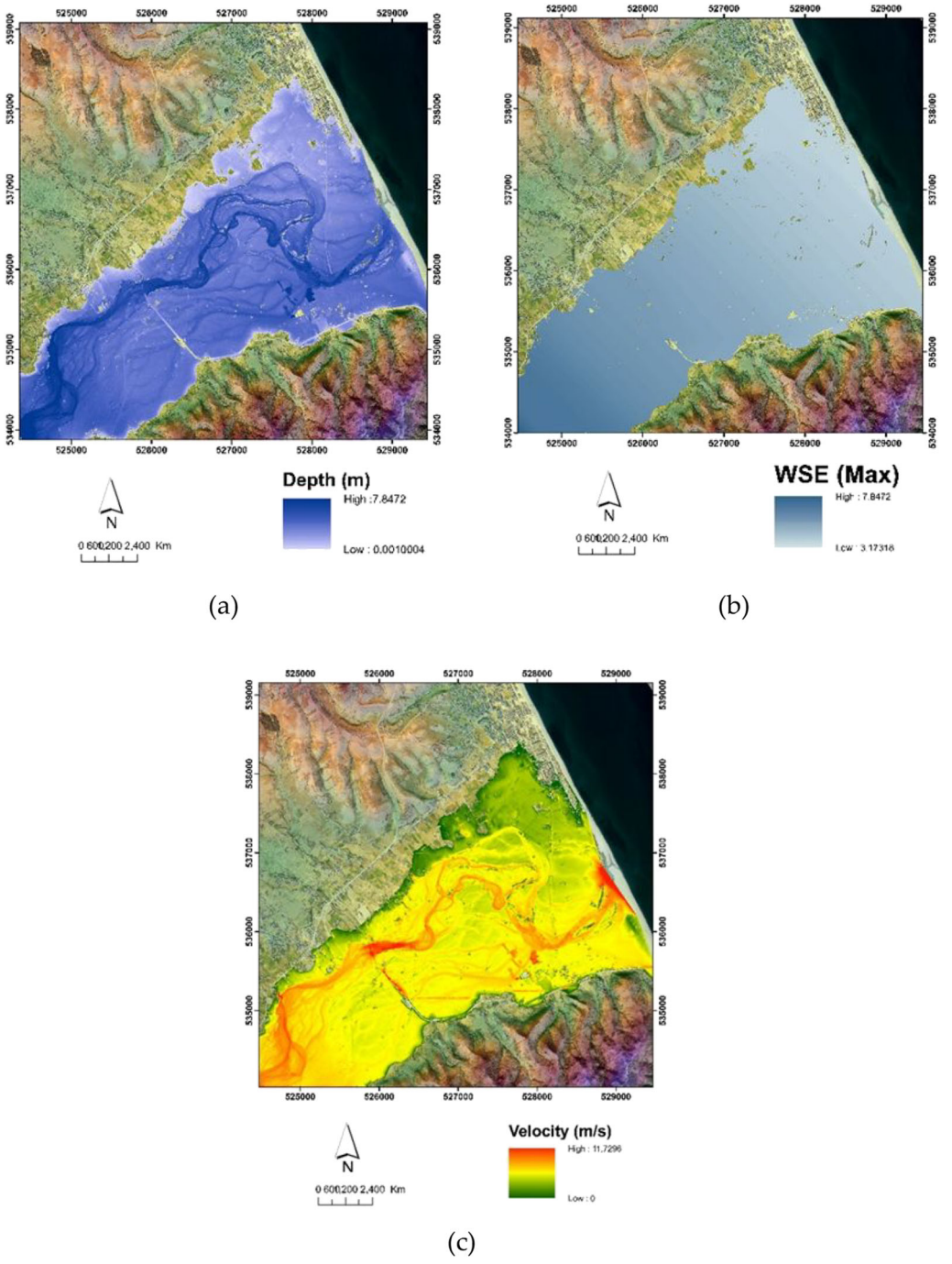

Figure 11. The 200-year recurrence flood model including water depth (a), WSE (b) and water Velocity (c).

quality of the mapping depends on the variation of the bathymetry. The higher this variation, the more accurate the prediction of wetlands. On one hand, bathymetry is a determining parameter, on the other hand, alone it could be the limitation of this method (TWI). When the topography is flat, the model tends to overestimate wetness. The TWI-

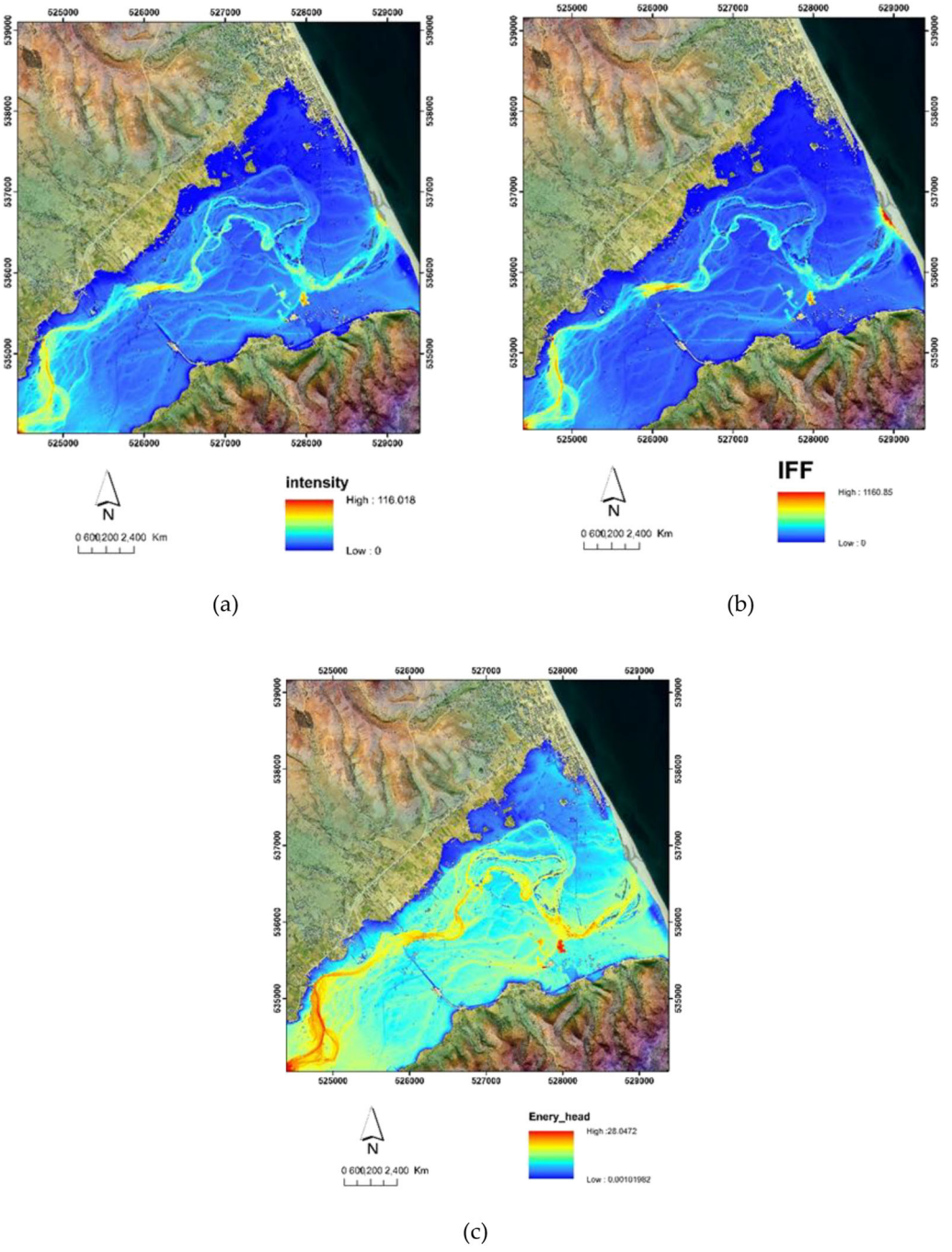

Figure 12. Map of flood indicators: Intensity (a), IFF (b) and Energy head (c).

Ks model makes proof of generating the correct wetness after integrating the hydraulic conductivity of the soil. Lastly, the topographical context was the perfect terrain that helped significantly to create this new model. Many watersheds in the world or sub-watersheds that are not gauged or the hydrological data are not always available. This model

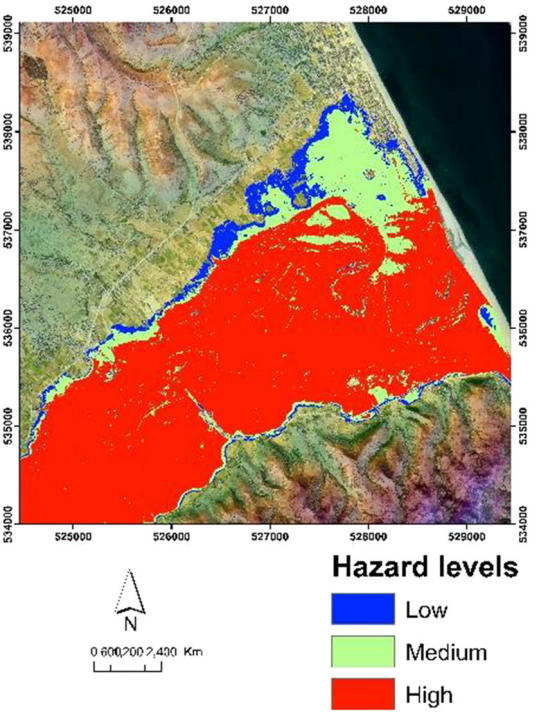

Figure 13. Map of Hazard level.

could be the relevant solution to provide an accurate prediction of flooded areas with limited input data and parametrization, especially without hydrological records. As well as less time for execution and calculation.

4.2. 2D Flood analyses at locale scale (the downstream floodplain)

The results obtained from the spatial simulation of a 200-year recurrence flood event using the 2D hydrodynamic model 'HEC-RAS' required: first, running the model under unstable flow conditions and inserting a runoff hydrograph of the maximum peak flow event that was recorded at the study site. Besides the integration of a high-resolution bathymetry (DTMs). This provided very detailed maps of the flood distribution in the plain. It was able to efficiently produce the spatial variation of flood depth, the entire flooded area/water surface elevation, and velocity propagation. Topography was a key factor in the process of velocity distribution, the extent of the flooded area over the main flow path, and water depths in and outside the channel.

The calculation and spatialization of flood indicators including Eh, IFF, I reflects that the concentration of the energy and intensity indicate significant damage are predicted in the middle part of the plain. This intensity distribution, Ehand IFF contribute and widely controls the mobilization of the lateral profile of the river due to the distribution of flow energy, sediment transport and consequently a long-term spatial modification of the areas under risk.

Many scientists have declared in the literature that 2D hydrodynamic models are competent to appropriately forecasting the following variables: water depth, velocity and flood extent on which decision-making regarding flood risk management is founded (Neelz and

Pender 2010, 2013; Teng et al. 2017). However, there are limitations related to the execution of these models. They work better in areas where natural reliefs are pronounced than flat bathymetry and therefore they have a tendency to forecast higher flood depths more precisely than shallow ones: indeed deep floodwaters are usually accumulated in areas of important variation of topography and where there are depressions in the surface of the landscape (Jamali et al. 2018).

The present research tried to challenge those limitations while simulating a nearly flat downstream area. Owing to the importance of this study. Floods are more damaging in the downstream than in the upstream. Many communities around the world are living around a river especially in the flood plain. This is the case of Oued Laou. Downstream of the watershed in this flat and urbanized plain surrounded by steep and mountainous hills. Producing a fine bathymetry datasets and choosing a small and limited area is important. Because the 2D models are generally considered as inaccurate for larger areas when the resolution requested is less than 10 m (Jamali et al. 2018). Which significantly helped to obtain accurate mapping because 2d HED-RAS is a computationally intensive model.

Many research works have stated that high-resolution terrain models provide more precise flood maps then low resolution DTMs that overestimate the water flood extents. The integration of a high-resolution DTM with centimetre-scale grid size in the model implementation is determinant but still not sufficient alone to declare that the model outcomes are reliable (Cook and Merwade 2009; Saksena and Merwade 2015; Sapountzis et al. 2021). It is unknown how the uncertainties associated with parameters and techniques, flood hydrographs, modelling and geospatial processing influence the total resolution of produced flood inundation maps (Quesada-Román et al. 2021). For this reason and in order minimize this related uncertainty, the use of the related under controlled inputs data such as high resolution DTM, real discharge records … can supply the capability to accurately anticipate areas exposed to flood inundation.

5. Conclusions

This study aims to assess and analyse flood risk in the Oued Laou basin by implementing two different and complementary approaches on two different spatial scales. The results of the previously determined objectives are summarized as follows:

5.1. Flood analyses on basin scale

Flood-prone areas were efficiently delineated using geomorphological models TWI/SAGA WI at the level of the Oued Laou basin. The areas downstream the basin, where topography is gentle, and the values of TWI are high (7–9), are most susceptible areas to flooding in the Oued Laou catchment. The new model called TWI-Ks was created based on the previous TWI by adding the hydraulic conductivity of the soil as a parameter. The results of all TWI /SAGA WI and TWI- Ks were compared in terms of the performance of prediction wetlands with real remotely sensed images. The TWI- Ks results gave a better delineation of areas prone to floods based on the previous comparison and realistic information, especially on the floodplain. Therefore, a better new version of TWI was successfully created. The effect of hydraulic conductivity was determinant to optimize the prediction of wetland and model performance. TWI-Ks is recommend for all types of watersheds. The proposed new model is an efficient tool, especially for ungauged rivers/basins, to identify and predict flood-prone areas.

5.2. Flood analyses on flood plain scale

In order to assess flood risk in a specific local area, which is most likely to be flooded is selected based on the geomorphological models, to proceed subsequently with a 2D HEC-RAS modelling. The conducted frequency analysis on a large historical data of instantaneous maximum discharge, through 10 different distributions. The occurrence of extreme flow rates has been estimated. Then the 200-year event (1800 m3) was selected for the 2D simulation based on the Pareto distribution.

Running a hydrodynamic model under a 2D routine using HEC RAS software makes it possible to produce an accurate flood mapping on a topographically flat plain. Indeed, the millimetre resolution of 30 cm of the elevation model, the instantaneous real flood hydrograph, and the optimum use of mesh grid size were important and determining to accurately generate flood extent. As well as estimate effectively the spatial variation of flood parameters, including water depth and velocity. In so far as the highest water elevation is estimated at 7.8 m. Flow indicators such as Eh, IFF, I are mapped. Showing that their high values are concentrated in the middle part of the floodplain where significant damage is predicted. Which coincides with the high hazard level.

The flood extent affected almost all settlements exposed on the flood plain including crop fields and road N16, it tends to present danger on buildings as well. Outcomes of this research can contribute greatly to flash flood damage mitigation. It is also a relevant document that adds to literature a new model TWI-Ks and resolve the problem of flat topography in 2 D hydrodynamic models. In addition, it will help decision-makers to efficiently manage flood risk in Oued Laou while taking into consideration the rapid expansion of urbanization.

Acknowledgements

We thank 'l'Agence Universitaire de la Froncophonie (AUF)' for the grant and the support of this work and the chance that gave us to communicate and collaborate with the Civil Engineering department of the Ovidius University Romania.

Disclosure statement

The authors declare no conflict of interest.

References

Afshari S, Tavakoly AA, Rajib MA, Zheng X, Follum ML, Omranian E, Fekete BM. 2018. Comparison of new generation low-complexity flood inundation mapping tools with a hydrodynamic model. J Hydrol 556:539–556.

Akaike H, Csaki, F, editors. 1973. Information theory and an extension of the maximum likelihood principle. In Petrov BN International Symposium on Information Theory, p. 267–281. References - Scientific Research Publishing. https://www.scirp.org/%28S%28vtj3fa45qm1ean45vvffcz55%29%29/reference/referencespapers.aspx?referenceid=1741007.

Alaghmand S, Abdullah R, Abustan I, Behdokht V. 2010. GIS-based river flood hazard mapping in urban area (A case study in Kayu Ara River Basin, Malaysia). Int J Eng Technol 2.

Amellah O, El Morabiti K. 2021. Assessment of soil erosion risk severity using GIS, remote sensing and RUSLE model in Oued Laou Basin (North Morocco). Soil Sci Ann 72(3):1–11.

Amellah O, El Morabiti K, Ouchar Al-djazouli M. 2020. Spatialization and assessment of flood hazard using 1D numerical simulation in the plain of Oued Laou (North Morocco). Arab J Geosci 13(14):635.

Anees MT, Abdullah K, Nawawi M, Norulaini N, Syakir MI, Kadir M. 2017. One- and two-dimensional hydrological modelling and their uncertainties. 2017 ISBN 978-953-51-3465-7.

Bărbulescu A, Maftei C. 2021. Statistical approach of the behavior of Hamcearca River (Romania). Rom Rep Phys 73(1):703.
Barling RD, Moore ID, Grayson RB. 1994. A quasi-dynamic wetness index for characterizing the spatial distribution of zones of surface saturation and soil water content. Water Resour Res 30(4):1029–1044.
Beven KJ, Kirkby MJ. 1979. A physically based, variable contributing area model of basin hydrology/un modèle à base physique de zone d'appel variable de l'hydrologie. Du Bassin Versant. Hydrol Sci Bull 24(1):43–69.
Böhner J, Selige T. 2002. Spatial prediction of soil attributes using terrain analysis and climate regionalization. Gottinger geograpihsche abhandlungen. Göttingen, Germany: Geographischen Instituts der Universität Göttingen.
Bomers A, Schielen RMJ, Hulscher SJMH. 2019. Hulsche SJM H. The influence of grid shape and grid size on hydraulic river modelling performance. Environ Fluid Mech 19(5):1273–1294.
Brunner GW. 2010. United states army; corps of engineers. Davis (CA): Institute for Water Resources (U.S.); Hydrologic Engineering Center (U.S.) HEC-RAS River Analysis System: Hydraulic Reference Manual; US Army Corps of Engineers, Institute for Water Resources, Hydrologic Engineering Center.
Buchanan BP, Fleming M, Schneider RL, Richards BK, Archibald J, Qiu Z, Walter MT. 2014. Evaluating topographic wetness indices across central New York agricultural landscapes. Hydrol Earth Syst Sci 18(8):3279–3299.
Burt T, Butcher D. 1986. Stimulation from simulation? A teaching model of hillslope hydrology for use on microcomputers. J Geograph Higher Educ 10(1):23–39.
Chow VT. 1959. Open-channel hydraulics. New York (NY): McGraw-Hill. ISBN 978-0-07-085906-7.
Colomina I, Molina P. 2014. Unmanned aerial systems for photogrammetry and remote sensing: a review. ISPRS J Photogramm Remote Sens 92:79–97.
Cook A, Merwade V. 2009. Effect of topographic data, geometric configuration and modeling approach on flood inundation mapping. J Hydrol 377(1–2):131–142.
Echeverribar I, Morales-Hernández M, Brufau P, Garcia-Navarro P. 2019. 2D numerical simulation of unsteady flows for large scale floods prediction in real time. Adv Water Resour 134:103444.
Erena SH, Worku H, De Paola F. 2018. Flood hazard mapping using FLO-2D and local management strategies of dire Dawa City, Ethiopia. J Hydrol Reg Stud 19:224–239.
Feng Q, Liu J, Gong J. 2015. Urban flood mapping based on unmanned aerial vehicle remote sensing and random forest classifier—A case of Yuyao, China. Water 7(12):1437–1455.
Forkuo EK. 2011. Flood hazard mapping using Aster image data with GIS. Int J Geomatics Geosci 1: 932–950.
Fustos I, Abarca-del-Rio R, Ávila A, Orrego RA. 2017. Simple logistic model to understand the occurrence of flood events into the Biobío River Basin in central Chile. J Flood Risk Manag. 10(1):17–29.
Gaume E, Bain V, Bernardara P, Newinger O, Barbuc M, Bateman A, Blaškovičová L, Blöschl G, Borga M, Dumitrescu A, et al. 2009. compilation of data on European flash floods. J Hydrol 367(1–2):70–78.
Geravand F, Hosseini SM, Ataie-Ashtiani B. 2020. Influence of river cross-section data resolution on flood inundation modeling: case study of Kashkan River Basin in Western Iran. J Hydrol 584:124743.
Granados-Bolaños S, Quesada-Román A, Alvarado GE. 2021. Low-cost UAV applications in dynamic tropical volcanic landforms. J Volcanol Geotherm Res 410:107143.
Guntner A, Seibert J, Uhlenbrook S. 2004. Modeling spatial patterns of saturated areas: an evaluation of different terrain indices. Water Resour Res40(5).
Hjerdt N, McDonnell J, Seibert J, Rodhe AA. 2004. New topographic index to quantify downslope controls on local drainage. Water Resour Res 40(5):W05602.
Jamali B, Löwe R, Bach PM, Urich C, Arnbjerg-Nielsen K, Deletic AA. 2018. Rapid urban flood inundation and damage assessment model. J Hydrol 564:1085–1098.
Keller T, Sutter JA, Nissen K, Rydberg T. 2012. Using field measurement of saturated soil hydraulic conductivity to detect low-yielding zones in three Swedish fields. Soil Tillage Res 124:68–77.
Kheradmand S, Seidou O, Konte D, Barmou Batoure MB. 2018. Evaluation of adaptation options to flood risk in a probabilistic framework. J Hydrol Reg Stud 19:1–16.
Komi K, Neal J, Trigg MA, Diekkrüger B. 2017. Modelling of flood hazard extent in data sparse areas: a case study of the oti River Basin, West Africa. J Hydrol Reg Stud 10:122–132.
Kossin JP. 2018. A global slowdown of tropical-cyclone translation speed. Nature 558(7708):104–107.
Kuha J. 2004. AIC and BIC: comparisons of assumptions and performance. Sociol Methods Res 33(2): 188–229.
Laio F, Di Baldassarre G, Montanari A. 2009. Model selection techniques for the frequency analysis of hydrological extremes. Water Resour Res. 45.

Langhammer J, Bernsteinová J, Miřijovský J. 2017. Building a high-precision 2D hydrodynamic flood model using UAV photogrammetry and sensor network monitoring. Water 9(11):861.
Maftei C, Papatheodorou K. 2015. Flash flood prone area assessment using geomorphological and hydraulic model. J Environ Prot Ecol 16:63–73.
Manfreda S, Di Leo M, Sole A. 2011. Detection of flood-prone areas using digital elevation models. J Hydrol Eng 16(10):781–790.
Marchi L, Borga M, Preciso E, Sangati M, Gaume E, Bain V, Delrieu G, Bonnifait L, PogacÌOEnik N. 2009. Comprehensive post-event survey of a flash flood in Western Slovenia: observation strategy and lessons learned. Hydrol Process23(26):n/a–3770.
Moore ID, Grayson RB, Ladson AR. 1991. Digital terrain modelling: a review of hydrological, geomorphological, and biological applications. Hydrol Process 5(1):3–30.
Neelz S, Pender G. 2010. Benchmarking of 2D dyfraulic modelling packages. Bristol: DEFRA/Environment Agency. https://www.gov.uk/government/uploads/system/uploads/attachment_data/file/290884/scho0510bsno-e-e.pdf.
Neelz S Pender G. 2013. Benchmarking the latest generation of 2D hydraulic modelling packages. Bristol: DEFRA/Environment Agency. http://evidence.Environmentagency.gov.uk/FCERM/Libraries/FCERM_Project_Documents/SC120002_Benchmarking_2D_hydraulic_models_Report.sflb.ashx.
O'Loughlin EM. 1986. Prediction of surface saturation zones in natural catchments by topographic analysis. Water Resour Res 22:794–804.
Oueslati A. 2008. Le littoral de Oued Laou de l'apport de l'étude géomorphologique à la connaissance de ses aptitudes à l'aménagement et à la prévention des risques naturels et de la dégradation des paysages. Travaux L'Inst Sci Rabat Sér Gén 5:1–16.
Papatheodorou K. 2015. Earthquake landslide and flood disaster prevention: the SciNetNatHaz project. Vol. 53.
Patel DP, Ramirez JA, Srivastava PK, Bray M, Han D. 2017. Assessment of flood inundation mapping of Surat city by coupled 1D/2D hydrodynamic modeling: a case application of the new HEC-RAS 5. Nat Hazards 89(1):93–130.
Pinos J, Timbe L. 2019. Performance assessment of two-dimensional hydraulic models for generation of flood inundation maps in mountain River Basins. Water Sci Eng 12(1):11–18.
Plate EJ. 2002. Flood risk and flood management. J Hydrol 267(1–2):2–11.
Pourali S, Arrowsmith C, Chrisman N, Matkan A, Mitchell D. 2016. Topography wetness index application in flood-risk-based land use planning. Appl Spatial Anal 9(1):39–54.
Qin C, Zhu AX, Pei T, Li B, Zhou C, Yang L. 2007. An adaptive approach to selecting a flow-partition exponent for a multiple-flow-direction algorithm. Int J Geograph Inform Sci 21(4):443–458.
Qin CZ, Zhu AX, Pei T, Li BL, Scholten T, Behrens T, Zhou CH. 2011. An approach to computing topographic wetness index based on maximum downslope gradient. Precision Agric 12(1):32–43.
Quesada-Román A, Villalobos-Portilla E, Campos-Durán D. 2021. Hydrometeorological disasters in urban areas of Costa Rica, Central America. Environ Hazard 20(3):264–278.
Quinn P, Beven K, Chevallier P, Planchon O. 1991. The prediction of hillslope flow paths for distributed hydrological modelling using digital terrain models. Hydrol Proc. 5:59–79.
Quirogaa VM, Kurea S, Udoa K, Manoa A. 2016. Application of 2D numerical simulation for the analysis of the February 2014 Bolivian Amazonia flood: application of the new HEC-RAS version 5. Ribagua 3(1):25–33.
Saksena S, Merwade V. 2015. Incorporating the effect of DEM resolution and accuracy for improved flood inundation mapping. J Hydrol 530:180–194.
Sanyal J, Lu XX. 2004. Application of remote sensing in flood management with special reference to monsoon Asia: a review. Nat Hazard 33(2):283–301.
Sapountzis M, Kastridis A, Kazamias AP, Karagiannidis A, Nikopoulos P, Lagouvardos K. 2021. Utilization and uncertainties of satellite precipitation data in flash flood hydrological analysis in ungauged watersheds. Glob Nest J. 23(3):388–399.
Schwarz G. 1978. Estimating the dimension of a model. Ann Statist 6(2):461–464.
Şerban G, Rus I, Vele D, Breţcan P, Alexe M, Petrea D. 2016. Flood-prone area delimitation using UAV technology, in the areas hard-to-reach for classic aircrafts: case study in the North-East of apuseni Mountains, Transylvania. Nat Hazard 82(3):1817–1832.
Smith JA. 1989. Regional flood frequency analysis using extreme order statistics of the annual peak record. Water Resour Res 25(2):311–317.
Sørensen R, Zinko U, Seibert J. 2006. On the calculation of the topographic wetness index: evaluation of different methods based on field observations. Hydrol Earth Syst Sci 10(1):101–112.

Teng J, Jakeman AJ, Vaze J, Croke BFW, Dutta D, Kim S. 2017. Flood inundation modelling: a review of methods, recent advances and uncertainty analysis. Environ Modell Softw 90:201–216.

Thapa S, Shrestha A, Lamichhane S, Adhikari R, Gautam D. 2020. Catchment-scale flood hazard mapping and flood vulnerability analysis of residential buildings: the case of Khando River in Eastern Nepal. J Hydrol Reg Stud 30:100704.

Van Oldenborgh GJ, Philip S, Kew S, van Weele M, Uhe P, Otto F, Singh R, Pai I, Cullen H, AchutaRao K. 2018. Extreme heat in India and anthropogenic climate change. Nat Hazards Earth Syst Sci18(1): 365–381.

Wang QJ. 1991. The POT model described by the generalized pareto distribution with poisson arrival rate. J Hydrol 129(1–4):263–280.

Yalcin E. 2020. Assessing the impact of topography and land cover data resolutions on two-dimensional HEC-RAS hydrodynamic model simulations for urban flood hazard analysis. Nat Hazards 101(3): 995–1017.

Yong B, Ren LL, Hong Y, Gourley JJ, Chen X, Zhang YJ, Yang XL, Zhang ZX, Wang WG. 2012. A novel multiple flow direction algorithm for computing the topographic wetness index. Hydrol Res 43(1–2): 135–145.

Zuhlke M, Fomferra N, Brockmann C, Peters M, Veci L, Malik J, Regner P. 2015. SNAP (sentinel application platform) and the ESA sentinel 3 toolbox. Sentinel-3 for Science Workshop. A work held 2–5 June, 2015 Venice, Italy. pp. 12–21.